



Technische Universität München

Chair of Media Technology

Prof. Dr.-Ing. Eckehard Steinbach

Bachelor Thesis

Refined Methods for Creating Realistic Haptic Virtual
Textures from Recorded Acceleration Data

Author:	Irem Öztürk
Matriculation Number:	03677343
Address:	Helene-Mayer-Ring 7A 80809 München
Advisor:	Matti Strese
Begin:	Datum des Arbeitsbeginns
End:	Datum des Vortrags

With my signature below, I assert that the work in this thesis has been composed by myself independently and no source materials or aids other than those mentioned in the thesis have been used.

München, September 27, 2018

Place, Date

Signature

This work is licensed under the Creative Commons Attribution 3.0 Germany License. To view a copy of the license, visit <http://creativecommons.org/licenses/by/3.0/de>

Or

Send a letter to Creative Commons, 171 Second Street, Suite 300, San Francisco, California 94105, USA.

München, September 27, 2018

Place, Date

Signature

Abstract

Several decades of research have been dedicated to the representation of real interactions in virtual or remote environments. Haptic interfaces give the possibility to touch virtual objects and to produce sensations during texture exploration by sliding a hand-held tool across a textured surface. This process elicits perceptual information about the properties of a texture based on the data recorded from real interactions. This thesis describes mathematical models for synthesizing acceleration signals at different velocities of a user during the surface exploration. These acceleration signals are then used for producing audio data to present microscopic roughness of a texture. The application of Linear Predictive Coding (LPC) is shown for interpolating between signals. Furthermore, computing recorded signals' major frequencies to predict acceleration data is introduced as another possible method for switching between audio recordings when the user's scanning speed changes. For both cases, high correlations are obtained between the predicted and recorded data without creating perceptually noticeable artifacts.

Contents

Contents	ii
1 Introduction	1
2 Haptic texture rendering	2
2.1 Roughness	2
2.1.1 Macroscopic Roughness	3
2.1.2 Fine Roughness	3
3 Interpolation of vibrotactile signals	4
3.1 Linear predictive coding	4
3.2 Signal Generation from Major Frequencies	6
4 Friction Dependence of Speed	11
4.1 Speed Test	11
4.2 Evaluation	11
5 Data-Driven Methods for Tactile Signal Evaluation	14
5.1 Experiment I	15
5.1.1 Subjects and Setup	15
5.1.2 Procedure	15
5.1.3 Results	16
5.1.4 Conclusion	16
6 Tactile Signal Speed Dependency Evaluation	17
6.1 Experiment II	17
6.1.1 Subjects and Setup	17
6.1.2 Procedure	17
6.1.3 Results	18
6.1.4 Conclusion	18
6.2 Beispiele für Referenzen	19
6.3 Schrifttypen	19
6.4 Archivierung	20

<i>CONTENTS</i>	iii
7 Zusammenfassung	21
A Ein Beispiel für einen Anhang	22
List of Figures	23
List of Tables	24
Bibliography	25

Chapter 1

Introduction

Scanning a textured surface with a tool generates rich high-frequency signals that demonstrate mainly microscopic roughness of a surface. These captured vibrations are called vibrotactile or acceleration signals which is considered synonymous as in [SHNS18]. To achieve full distal attribution, sensed vibrations must correspond to the user inputs in a physically appropriate manner [Loo92].

A reasonable idea is that varying one's exploratory speed and normal force must significantly alter the realism. However, studies (e.g. [CK15]) show that removing force responsiveness does not have a significant effect on the perceived realism, whereas removing speed responsiveness is more salient to users. Therefore, vibration signals in this thesis include speed responsiveness and not force responsiveness.

Allowing texture vibrations to respond to user speed is a valuable part of creating realistic haptic textures, nonetheless can be a challenging and time consuming part of the implementation, if real recorded acceleration signals are displayed for every speed level. Some research [JMRK10] elucidate mathematical models as an alternative solution for representing a vibration texture under specific probe-surface interaction conditions.

This thesis has fine texture features as its center of focus and aims to evaluate the prediction results obtained from mathematical models, namely LPC and major frequency analysis to be able to display realistic vibrations at different speed levels through interpolated audio signals.

Chapter 2

Haptic texture rendering

The human haptic perception system relies on kinesthetic and cutaneous sensory information provided by several receptors during probe-surface interactions [LK09].

The kinesthetic sense focuses on the perception of forces and torques acting on the human body. Kinesthetic stimulation is sensed by mechanoreceptors located in the muscles. Kinesthetic mechanoreceptors include muscle spindles in parallel with muscle fibers and Golgi tendon organs in series with them at the connection with the skeleton [Cha15]. In some mainly kinesthetic tasks, the tactile sense only indicates a contact.

Tactile perception is stimulated by cutaneous receptors. There are four kinds of mechanoreceptors in the glabrous skin: The Merkel cells (Braille dots and sharp edges), Meissner corpuscles (low-frequency vibrations), Pacinian corpuscles (high frequency stimuli), Ruffini endings (still unknown).

Friction, hardness, macroscopic roughness, microscopic roughness and thermal conductivity are the main dimensions to build haptic texture models. All of these aspects should be well considered in order to increase immersion into a virtual environment. In the following of this thesis, microscopic roughness is our main focus as a vibrotactile feature.

2.1 Roughness

As an abstract feature roughness plays an important role in haptic signal perception. The roughness dimension may be divided into two dimensions: macro and fine (micro) roughness as in [SOY13].

2.1.1 Macroscopic Roughness

Due to the duplex nature of roughness, macroscopic roughness should strictly be considered in order to understand fine roughness. Coarse roughness is mainly represented by the “uneven”, “relief”, or “voluminous” labels and mediated by different mechanisms from micro roughness. For coarse surface roughness, the spatial distribution of SAI units is related to roughness perception [SOY13].

2.1.2 Fine Roughness

In the mechanism of fine roughness perception, FAI and FAII units contribute and is mainly represented by the “rough” label. During surface-tool or surface-finger sliding motions, high frequency vibrations can be extracted using an accelerometer mounted on a human finger. Microscopic roughness impressions can be characterized by these vibrations. The macro and fine roughness dimensions can be separated according to the mentioned aspects but can intersect each other during the process of perception. Figure 2.1 illustrates the process of texture production with an accelerometer.

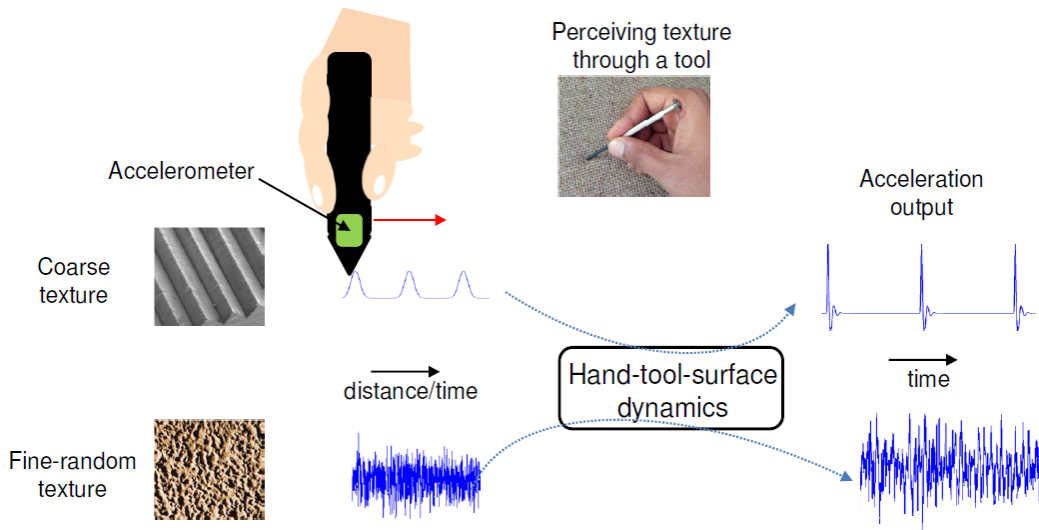


Figure 2.1: Mechanism of texture production. A hand-held tool is used to stroke a textured surface. An acceleration sensor signal mounted on the tool measures the response of the hand-tool system as it hits surface features. Figure reproduced from [Cha15]

The recorded acceleration signals depend on the scan speed and force, nonetheless we ignore the force dependencies as mentioned in the introduction part. Thereby, our approach in this thesis is generating vibrotactile signals based on the recorded acceleration data for different absolute scan speed. They are then displayed via a voice coil actuator.

Chapter 3

Interpolation of vibrotactile signals

Priori model designs have recently been evolved into data-driven haptic textures. The apparent concept is simply displaying recorded texture acceleration signals, where the exploratory speed dependency is disregarded. However, this is not a sufficient way of representing acceleration response. Therefore, user speed should be incorporated into the feedback signal.

As in [CRC⁺12] is described, there are some methods of relating speed variable to tactile signals such as switching between recordings according to speed, which may however be perceptually detectable. Another way is building a function depending on speed that gives a weighted average of recorded acceleration signals as output. The problem that may occur here is that the frequency content is not preserved due to the probable constructive and destructive interference between signals. These aspects create the idea of data-driven texture models.

In the following, we analyze two methods for synthesizing vibrotactile signals without creating noticeable artifacts. The first method is synthesizing two recorded acceleration signals under different speed conditions through LPC method and interpolating between them by linear interpolation of filter variables. The second one is reproducing these two signals from their major frequencies and interpolating between them according to the major frequencies.

In the following, we go deep into both of the principles and how to apply them to produce interpolated signals.

3.1 Linear predictive coding

The basic idea of Linear Predictive Coding (LPC) is to develop a transfer function that can predict each sample of a signal as a linear combination of the previous samples. It has

applications in filter design and speech coding.

We consider an IIR filter $H(z)$ of length n in the form $H(z) = [-h_1z^{-2} - h_2z^{-1} \dots - h_nz^{-n}]$. Our acceleration data vector from PCA is called $\vec{a}(k)$ in the following. The resulting prediction vector from our filter is $\vec{\hat{a}}(k)$. The residual signal $\vec{e}(k)$ is the difference between these two signals. The transfer function $P(z)$ is the result of the following equation:

$$\frac{\vec{e}(k)}{\vec{a}(k)} = 1 - H(z) = P(z) \quad (3.1)$$

It is possible to compute the residual at each step using the vector of filter coefficients $\vec{h} = [h_1 h_2 h_3 \dots h_n]^T$:

$$\vec{e}(k) = a(k) - \hat{a}(k) = a(k) - \vec{h}^T \vec{a}(k-1) \quad (3.2)$$

At this step, we aim to find the minimum value of the residual function $e(k)$. We are able to reduce the problem to Wiener-Hopf equation by a cost function based on mean-square error. The Wiener-Hopf equation can be solved by Levinson-Durbin [Dur60] algorithm, so that we can obtain our optimal filter vector \vec{h}_0 .

To synthesize new signals, we use a white noise signal $\vec{e}_g(l)$ as input, which is filtered with $1/P(z)$, in order to generate our desired response $\vec{a}_g(l)$. For a better overview, we can rewrite the equations (3.1) and (3.2) as follows:

$$\frac{\vec{a}_g(l)}{\vec{e}_g(l)} = \frac{1}{1 - H(z)} = \frac{1}{P(z)} \quad (3.3)$$

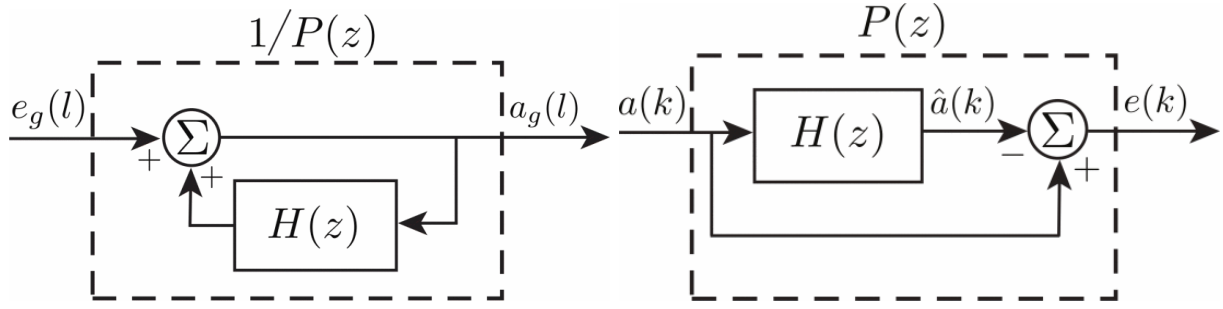
$$a_g(l) = e_g(l) + \vec{h}^T \vec{a}_g(l-1) \quad (3.4)$$

Figure 3.1 illustrates each of analyzing and synthesizing processes via block diagram. The value $\vec{e}_g(l)$ is a randomly generated Gaussian white noise but its average signal power must be equal to that of the average signal power remaining in the residual, $P\{\vec{e}(k)\}$ after filter optimization.

The definition of power is as in the following equation:

$$P\{\vec{a}(l)\} = \frac{1}{N} \sum_{n=0}^{N-1} |a(n)|^2 \quad (3.5)$$

This is equivalent to signal variance σ^2 , because our signals are zero-mean signals. Now, we have to determine the order of our prediction filter, which affect the accuracy of the prediction. The higher we choose the order, the smaller the residual gets. It means we have



(a) Block diagram for prediction of the next contact acceleration signal $a_g(l)$ from the appropriately scaled white noise input $e_g(l)$. (b) Block diagram for the synthesis of an acceleration signal $a(k)$ given the recorded series $a(k)$ with noise input $e_g(l)$.

Figure 3.1: Signal generation through LPC principle. Figures reproduced from [JMRK10].

a better prediction with higher orders, but then the calculation gets more complicated. It is possible to calculate the success of the synthetic result with a cost function defined as the RMS error as follows:

$$C\{\vec{a}_g(l)\} = \frac{RMS(DFT_s\{\vec{a}(l)\} - DFT_s\{\vec{a}_g(l)\})}{RMS(DFT_s\{\vec{a}(l)\})} \quad (3.6)$$

Using this equation, where $DFT_s\{\vec{a}\}$ represents the discrete Fourier transform of vector \vec{a} , it is possible to obtain the optimal order of the filter. In our case we choose 400 as the order for the best quality of results as in [JMRK10].

Now that we have generated our prediction filter with two unique variables \vec{h} vector and $e_g(l)$, it comes to interpolate between our synthesized signals to create new signals. Bilinear interpolation of both the vector \vec{h} and $e_g(l)$ of two signals in different velocities and applying these new values to our prediction filter result in new synthesized signals, so that we create signal data for audio signals at different force and velocities. For the interpolation of filter coefficients, we first convert them to line spectral frequencies (LSFs) to ensure stability during rendering [HC14].

3.2 Signal Generation from Major Frequencies

The other method for signal generation is using rich and valuable information of signals' dominant frequencies, which has the highest amplitudes. The frequency of the vibration must change as the users change their force and so that their velocity. This is one of the realistic methods for interpolation between signals recorded under different velocities.

At first we should determine the number of the frequencies we are going to deal with for synthesizing new signals. This is done as the part of our first experiment according to

the participants' feedback. For our case we set 30 as the maximum number of selected frequencies and 2 as the minimum. The optimum will be evaluated with the aid of the first experiment.

In order to find the frequencies with highest amplitudes, we calculate the discrete Fourier transform of the two recorded data and then select highest amplitudes of the transformed signals. It is important here to ensure that selected frequencies should have a certain distance to each other, because the superposition of two pure tones with slightly different frequencies can lead to beats. To avoid this phenomenon, we remove frequencies among selected ones with a small difference.

The threshold difference that the frequencies should have among each other is called "just noticeable difference (JND)". As described in [Cha15],

In Figures 3.2 and 3.3, an example of coak material is shown to illustrate how the artificial signal is generated from the recorded data. The signal is recorded at a very slow scanning speed (50mm/s) on coak and the obtained three-axis time-domain signals are reduced to one-axis using DFT321 [JMR12]. The generated signal from selected frequencies is in Figure 3.4 both in time and spectral domain.

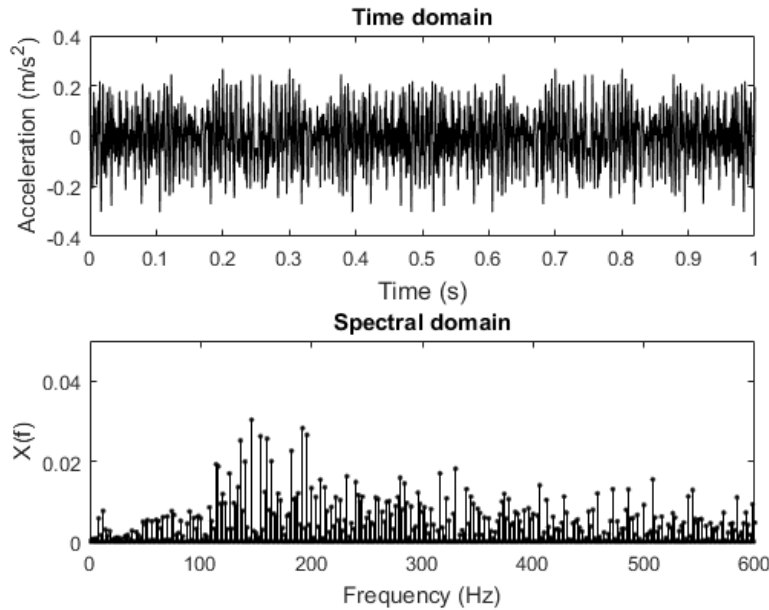


Figure 3.2: The depicted signal is recorded during an interaction with coak at a speed of 50 mm/s. The first plot shows the reduced one-axis signal in time domain and second plot shows spectral properties of the signal.

The remaining frequencies of the recorded signals are utilized as skeleton of new signals to be generated. We define the frequency, the angle and the amplitude of each selected sample.

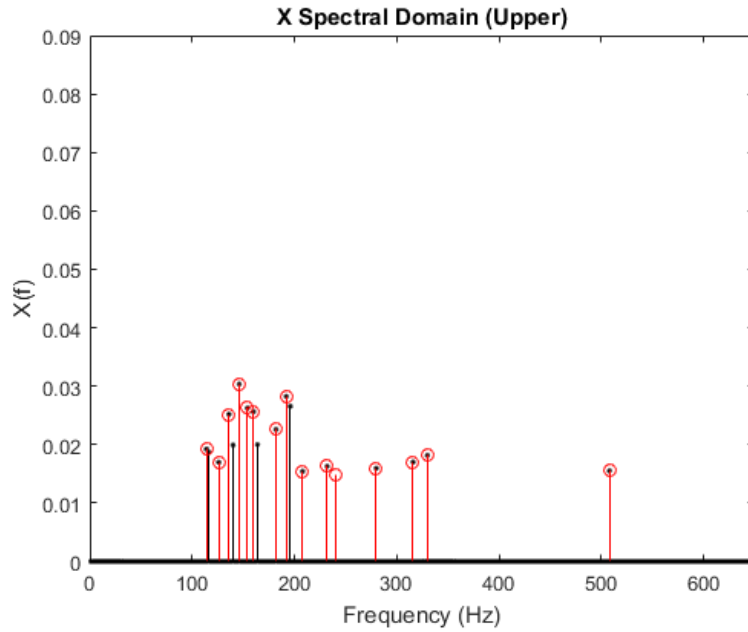


Figure 3.3: As an example, here is the number of selected frequencies 20 and the threshold difference is 5. The red points show the remaining 15 frequencies and the black ones are with 0.5 and above amplitudes, so that the upper side of the spectral domain is given with selected frequencies for a better overview.

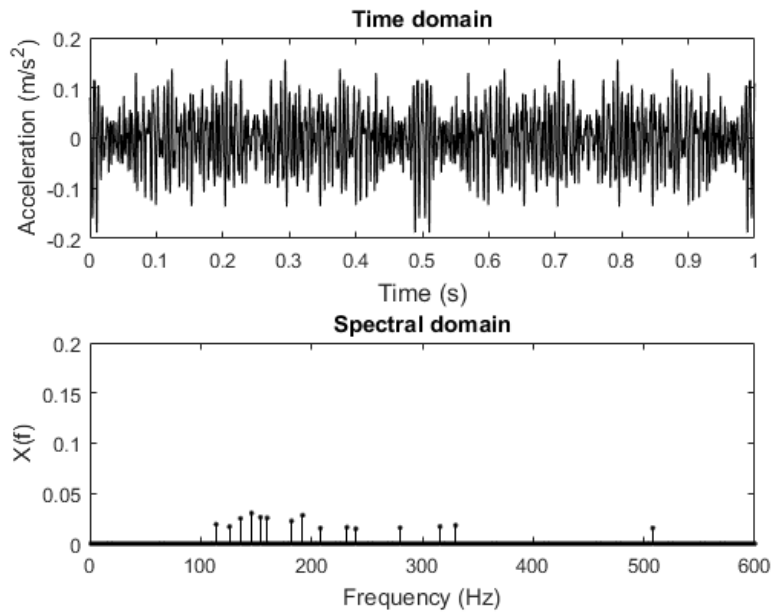
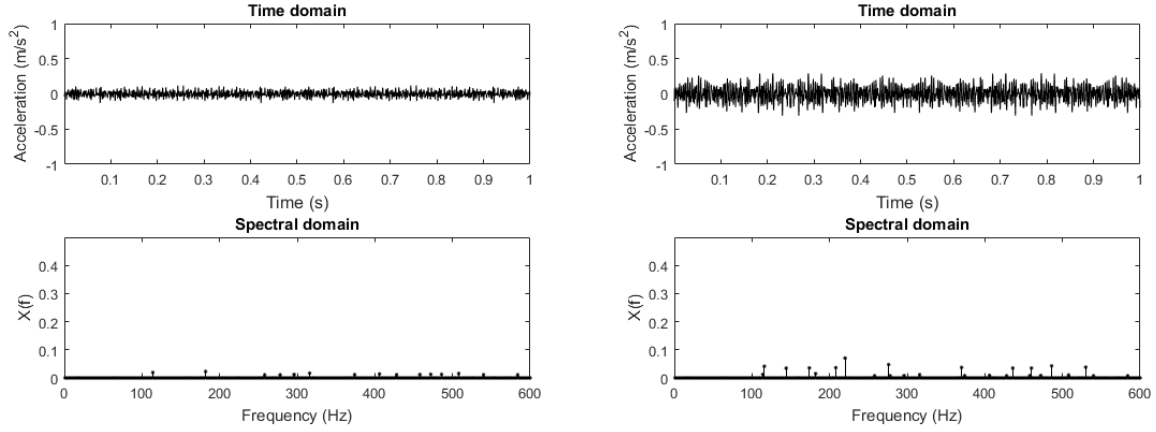


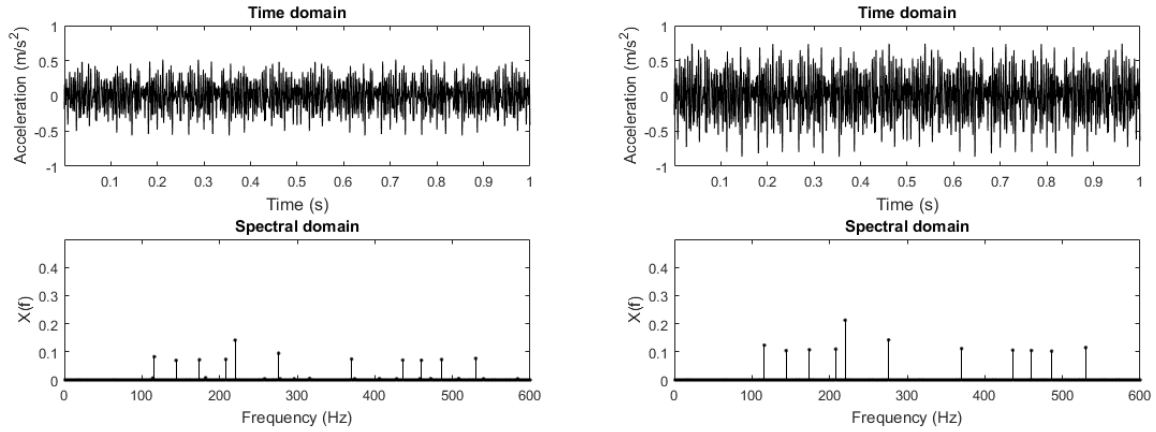
Figure 3.4: First plot is the time domain of the generated signal via the frequencies in the second plot, which were chosen in Figure 3.3.

We synthesize new signals by applying linear interpolation to the selected frequencies' amplitudes (see Figure 3.5) and new signals are generated according to the following equation:

$$z = z + \max A(k) * (\cos(2 * \pi * t * \max F(k) + \max P(k)) + i * \sin(2 * \pi * t * \max F(k) + \max P(k))) \quad (3.7)$$



(a) First generated signal from recorded data at speed 50mm/s reproduced from given frequencies below. (b) In this example, between two recorded data at different speed two signals are interpolated. Here, the first result of interpolation is shown.



(c) Second result of the interpolation. Combination of the frequencies can be seen in the spectral domain plot below. (d) The reproduced signal from recorded data at speed 400mm/s reproduced from given frequencies below.

Figure 3.5: Signal interpolation through frequencies with highest amplitudes.

where $\max A(k)$ represents the amplitude of selected frequencies and $\max F(k)$ the frequency, $\max P(k)$ represents the phase of selected frequencies. Signal z is zero initialized at the beginning and updated as long as a new value of frequency exists.

Finally in both methods, we write audio data by *audiowrite* function in Matlab using the estimated signals.

Chapter 4

Friction Dependence of Speed

Surface stickiness compels the users to apply a lateral force during surface interactions. The friction coefficient is usually calculated as the ratio of the required dragging force of a sensor to the pressure, or normal force [SHNS18].

4.1 Speed Test

In the following, we use a Phantom Omni device to feel a surface with different friction conditions, to be able to create a speed scala for some friction coefficients. Our aim is demonstrating how user speed varies depending on friction coefficients. We then use these results to evaluate speed intervals to be created in the following of this thesis, in which different audio data is displayed.

The test is carried out with an object in a haptic virtual environment, which has no friction at the beginning. The scanning speed is detected and saved in every 0.2 seconds, while the user explores the surface. Approximately after one minute, system automatically changes the friction and brings it to one level higher. The friction coefficients and the results are shown in Figures 4.1 and 4.2.

4.2 Evaluation

Figure 4.1 presents the mean speed value and the common speed interval for each coefficient order. As expected, both the speed interval and the mean value get smaller with increasing friction coefficient. Figure 4.2 gives us hints to be able to analyze how many intervals there are to display different audio data to simulate real surfaces.

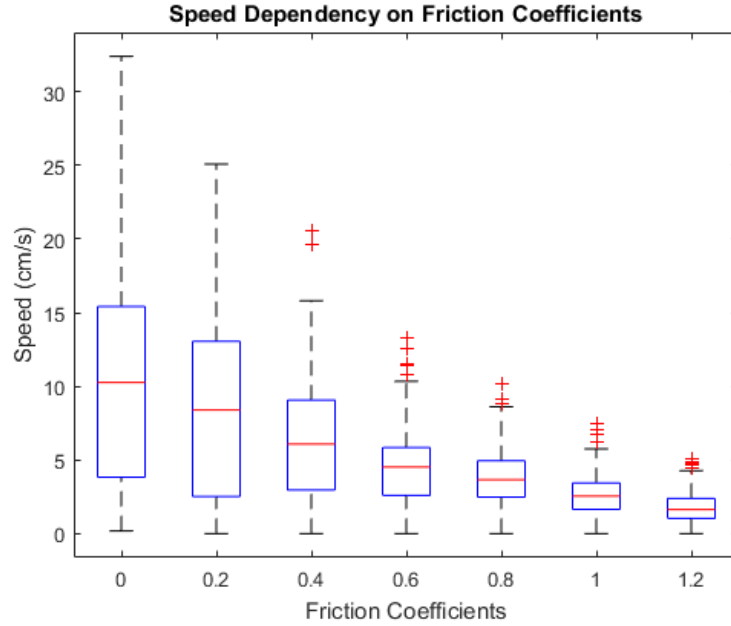


Figure 4.1: Boxplot between friction coefficients of a virtual surface and speed values detected in every 0.2 seconds.

In plot (a), nine bins are shown, where the last two can be ignored due to the small number. So in that case, we would choose seven intervals for changing audio as the user speed varies, on the other hand in real life, textures always have a friction above zero, so this example depicts an unnatural scenario. When we look at the most common coefficients like 0.2 and 0.4, which are also relevant for the experiments in following chapters, we recognize that, it is possible to work with less than seven intervals for vibrotactile response. In the case of 0.2, five bins are remarkable as peaks and the rest can be part of the last interval. For the friction 0.4, we can assign four intervals and for 0.6 three audio data are quite sufficient. The fine roughness of objects with 0.8 and 1.0 friction coefficient can be displayed with two signals and for the last and extreme case one audio is enough already according to the presented results, so that there is no need to interpolate the recorded data.

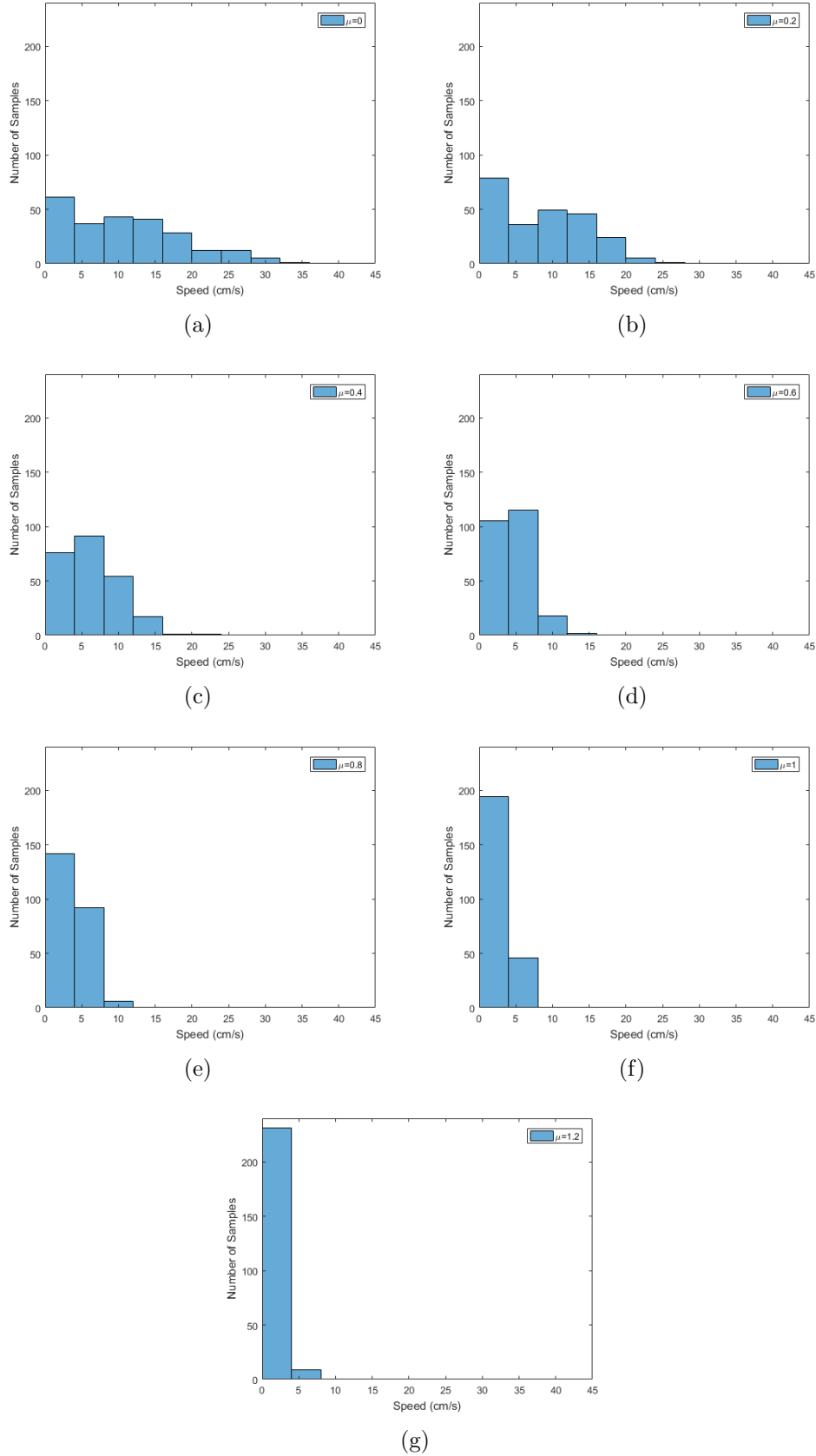


Figure 4.2: Histograms of each 7 friction coefficients with 240 speed samples saved in every 0.2 seconds during virtual surface interaction through a haptic device. The bin width is selected as 4 in each plot.

Chapter 5

Data-Driven Methods for Tactile Signal Evaluation

The perception of displayed haptic information typically varies across different human subjects [LK09]. Therefore, experiments with human participants and their feedbacks constitute a fundamental component of the development in haptics.

As mentioned in chapter 3, we analyze two methodologies of synthesizing vibrotactile signals for rendering fine roughness feedback: LPC and utilizing major frequencies of records. This chapter describes a human-subject experiment to evaluate how perceptually close our synthesized vibrotactile signals to the recorded acceleration signals in a haptic environment.

Before the experiment, spectral analysis of a recorded and its synthesized version via both methodology is given as a sample in Figure ?.

–figure

The general feel of haptic textures is governed by their spectral signature [KJKM11]. As in the figure ?, the recorded and synthesized data differ on time-domain, but their spectrum are quite similar. So it is expected that they will feel the same to a user. Whether these correlations are strong enough to fool the human sense of touch were planned to investigate in [JMRK10], which Experiment I is going to deal with in the next section.

5.1 Experiment I

5.1.1 Subjects and Setup

To accomplish a stable evaluation, ten volunteer human subjects, 3 female and 7 male, participated in the experiment at separate times. Their ages ranged from 19 to 29, with an average of 23 years. The subjects were all right-handed with limited experience with haptic devices. None of them reported having any ailments that would affect the experiment.

We used the voice coil actuator model NCC01-04-001-1X by H2W Technologies in the experiment to display vibrotactile signals. 5 objects were relevant for this experiment as shown in the tabular 5.1.

Table 5.1: Materials in the experiment given with their approximated friction coefficients.

Material	Friction
Coarse foam	0.6
Fine foam	0.6
Coak	0.2
Granite Tile	0.2
Steel wool	0.4

5.1.2 Procedure

The subject sat at a table in front of the voice coil actuator. In each experiment run, the subject compared a synthesized signal with the reference while perceiving the response with the right index finger. The displayed reference signal was for each material a recorded acceleration data and the compared synthesized signal was reproduced from this data both via LPC and major frequency method.

In addition to these synthesized signals, the signal obtained by converting the initial signal from time domain to frequency domain via DFT and then converting back from the frequency domain to the time domain via IFFT was also displayed to be compared with the reference by the participants. The intent here is to remove possible peculiarities that may have occurred at the beginning and end of the recording and so that providing a stable signal from the recording.

The subject was supposed to compare each pair of signals respectively and evaluate whether they cause the same or different perception. Before each synthesized signal, the recorded signal is displayed for 20 seconds. Afterwards the artificial produced audio is displayed again for 20 seconds and the participant was asked to evaluate directly. Hereby, all methods were judged regarding to the reference.

This setting was repeated for each 5 materials and an experiment run was terminated after the subject judged the signal pairs to feel the “same” or “different” for each material.

5.1.3 Results

–kim ne dedi burda ver ama sonuclari conclusionda degerlendir?

5.1.4 Conclusion

Chapter 6

Tactile Signal Speed Dependency Evaluation

lpc uses the autocorrelation method of autoregressive (AR) modeling to find the filter coefficients.

6.1 Experiment II

The four virtual surfaces were created by altering the texture vibrations? responsiveness to user force and speed. The

6.1.1 Subjects and Setup

from dragging a Phantom Omni across a textured surface [9]. They recorded the spectrum for two tangential speeds and in-

6.1.2 Procedure

Subjects were also given time to practice using the Omni by exploring a simple haptic environment consisting of a sphere and cube inside of a box.

6.1.3 Results

6.1.4 Conclusion

— Von Quellen:

We explain how to apply the mathematical principles of Linear Predictive Coding (LPC) to develop a discrete transfer function that represents the acceleration response under specific probe-surface interaction conditions. We then use this predictive transfer function to generate unique acceleration signals of arbitrary length. In order to move between transfer functions from different probe-surface interaction conditions, we develop a method for interpolating the variables involved in the texture synthesis process. Finally, we compare the results of this process with real recorded acceleration signals, and we show that the two correlate strongly in the frequency domain.

These vibrations depend on the motions of the tool and respond to both normal force and tangential speed. This paper explores various methods of simulating haptic texture interactions by rendering tool vibrations that are based on recorded data. We designed and ran a human-subject study (N=15) to analyze the importance of creating virtual texture vibrations that respond to user force and speed. Our analysis of data from fifteen textures showed that removing speed responsiveness did cause a statistically significant decrease in perceived realism, but removing force responsiveness did not. This result indicates that virtual textures aiming to simulate real surfaces should vary the rendered vibrations with user speed but may not need to vary them with user force. that represents the acceleration response under specific probe- surface interaction conditions.

statistically significant decrease in realism this study elucidated the conditions necessary to create realistic haptic textures. a process of synthesizing probe-surface interactions from data recorded from real interactions. via automated analysis of real recorded data. While haptic feedback is known to increase the immersion into a virtual environment (VE), most haptic feedback devices lack the ability to display multidimensional tactile impressions. To provide a more efficient and robust method of building haptic texture models from tool-surface interaction data...

$$mRG = \beta \cdot \sum_{k=1}^K \sum_{l=1}^L \hat{\mathbf{X}}(k, l) \quad (6.1)$$

Durch die \label kann auf die Bilder mit \ref verwiesen werden.

6.2 Beispiele für Referenzen

Die Literaturhinweise werden im Text z.B. folgendermaßen verwendet:

“..., wie in gezeigt, ...” oder “... es gibt mehrere Ansätze [Arn99, GLL90] ...”

6.3 Schrifttypen

Als Schrifttyp wird Arial oder Roman empfohlen. Bitte beachten, daß Größen und Einheiten eine eigene Schreibweise haben:

Kursivschrift: physikalische Größen (z.B. U für Spannung), Variablen (z.B. x), sowie Funktions- und Operatorzeichen, deren Bedeutung frei gewählt werden kann (z.B. $f(x)$)

Steilschrift: Einheiten und ihre Vorsätze (z.B. kg, pF), Zahlen, Funktions- und Operatorzeichen mit feststehender Bedeutung (z.B. sin, lg)

6.4 Archivierung

Für die Archivierung sind alle Dateien der Arbeit (auch der Vorträge) dem Betreuer zur Verfügung zu stellen. Weiterhin soll noch ein BibTeX-Eintrag der Arbeit erstellt werden (die Felder in eckigen Klammern sind dabei auszufüllen):

```
@MastersThesis{<Nachname des Autors><Jahr>,  
  type =          {<Art der Arbeit>},  
  title =         {{<Thema der Arbeit>}},  
  school =        {Institute of Communication Networks~(LKN),  
                   Munich University of Technology~(TUM)},  
  author =        {<Nachname des Autors>, <Vorname des Autors>},  
  annote =        {<Nachname des Betreuers>, <Vorname des Betreuers>},  
  month =         {<Monat>},  
  year =          {<Jahr>},  
  key =           {<Mehrere Suchschlüssel>}  
}
```

Chapter 7

Zusammenfassung

Am Schluß werden noch einmal alle wesentlichen Ergebnisse zusammengefaßt. Hier können auch gemachte Erfahrungen beschrieben werden. Am Ende der Zusammenfassung kann auch ein Ausblick folgen, der die zukünftige Entwicklung der behandelten Thematik aus der Sicht des Autors darstellt.

Appendix A

Ein Beispiel für einen Anhang

Beispiel für eine Tabelle:

Table A.1: Beispiel für eine Beschriftung. Tabellenbeschriftungen sind üblicherweise über der Tabelle platziert.

left	center	right
entry	entry	entry
entry	entry	entry
entry	entry	entry

List of Figures

2.1	Mechanism of texture production. A hand-held tool is used to stroke a textured surface. An acceleration sensor signal mounted on the tool measures the response of the hand-tool system as it hits surface features. Figure reproduced from [Cha15]	3
3.1	Signal generation through LPC principle. Figures reproduced from [JMRK10].	6
3.2	The depicted signal is recorded during an interaction with coak at a speed of 50 mm/s. The first plot shows the reduced one-axis signal in time domain and second plot shows spectral properties of the signal.	7
3.3	As an example, here is the number of selected frequencies 20 and the threshold difference is 5. The red points show the remaining 15 frequencies and the black ones are with 0.5 and above amplitudes, so that the upper side of the spectral domain is given with selected frequencies for a better overview.	8
3.4	First plot is the time domain of the generated signal via the frequencies in the second plot, which were chosen in Figure 3.3.	8
3.5	Signal interpolation through frequencies with highest amplitudes.	9
4.1	Boxplot between friction coefficients of a virtual surface and speed values detected in every 0.2 seconds.	12
4.2	Histograms of each 7 friction coefficients with 240 speed samples saved in every 0.2 seconds during virtual surface interaction through a haptic device. The bin width is selected as 4 in each plot.	13

List of Tables

5.1	Materials in the experiment given with their approximated friction coefficients.	15
A.1	Beispiel für eine Beschriftung. Tabellenbeschriftungen sind üblicherweise über der Tabelle platziert.	22

Bibliography

- [Arn99] B. St. Arnaud. Gigabit Internet to every Canadian Home by 2005. <http://www.canet2.net/archeng/home.html>, 1999.
- [Cha15] Rahul Gopal Chaudhari. *Data Compression and Quality Evaluation for Haptic Communications*. PhD thesis, Technische Universitat Munchen, 2015.
- [CK15] Heather Culbertson and Katherine J. Kuchenbecker. Should haptic texture vibrations respond to user force and speed? In *IEEE World Haptics Conference*, pages 106 – 112, Evanston, Illinois, USA, June 2015. Oral presentation given by Culbertson.
- [CRC⁺12] H. Culbertson, J. M. Romano, P. Castillo, M. Mintz, and K. J. Kuchenbecker. Refined methods for creating realistic haptic virtual textures from tool-mediated contact acceleration data. In *2012 IEEE Haptics Symposium (HAPTICS)*, pages 385–391, March 2012.
- [Dur60] J. Durbin. The fitting of time-series models. *Revue de l’Institut International de Statistique / Review of the International Statistical Institute*, 28(3):233–244, 1960.
- [GLL90] J. S. Griswold, T. L. Lightle, and J. G. Lovelady. Hurricane Hugo: Effect On State Government Communications. *IEEE Communications Magazine*, 28(6):12–17, 1990.
- [HC14] Katherine J. Kuchenbecker Heather Culbertson, Juliette Unwin. Modeling and rendering realistic textures from unconstrained tool-surface interactions. *IEEE Transactions on Haptics*, 7(3):381–393, 2014.
- [JMR12] K. J. Kuchenbecker J. M. Romano. Creating realistic virtual textures from contact acceleration data. *IEEE Transactions on Haptics*, 5(2):109–119, 2012.
- [JMRK10] Takashi Yoshioka Joseph M. Romano and Katherine J. Kuchenbecker. Automatic filter design for synthesis of haptic textures from recorded acceleration data. In *Proceedings, IEEE International Conference on Robotics and Automation*, pages 1815–1821, May 2010.

- [KJKM11] J. M. Romano K. J. Kuchenbecker and W. McMahan. Haptography: Capturing and recreating the rich feel of real surfaces. In Cédric Pradalier, Roland Siegwart, and Gerhard Hirzinger, editors, *Robotics Research*, pages 245–260, Berlin, Heidelberg, 2011. Springer Berlin Heidelberg.
- [LK09] S. J. Lederman and R. L. Klatzky. Haptic perception: A tutorial. *Attention, Perception, & Psychophysics*, 71(7):1439–1459, 2009.
- [Loo92] J. M. Loomis. Distal attribution and presence. *Presence: Teleoperators and Virtual Environments*, 1(1):113–119, 1992.
- [SHNS18] Matti Strese, Rania Hassen, Andreas Noll, and Eckehard Steinbach. A tactile computer mouse for the display of surface material properties. PP(99):1–1, 08 2018.
- [SOY13] H. Nagano S. Okamoto and Y. Yamada. Psychophysical dimensions of tactile perception of textures. *IEEE Transactions on Haptics*, 6(1):81–93, 2013.